Cooper-pair-based photon entanglement without isolated emitters

Alex Hayat,[1] Hae-Young Kee,[2,3] Kenneth S. Burch,[2,3,4,5] and Aephraim M. Steinberg[2,4]
[1]*Department of Electrical Engineering, Technion, Haifa 32000, Israel*
[2]*Department of Physics, University of Toronto, Toronto, Ontario, Canada M5S 1A7*
[3]*Centre for Quantum Materials, University of Toronto, 60 St. George Street, Toronto, Ontario, Canada M5S 1A7*
[4]*Centre for Quantum Information and Quantum Control and the Institute for Optical Sciences, University of Toronto, 60 St. George Street, Toronto, Ontario, Canada M5S 1A7*
[5]*Department of Physics, Boston College, 140 Commonwealth Avenue, Chestnut Hill, MA 02467, USA*
(Received 25 April 2013; revised manuscript received 30 January 2014; published 10 March 2014)

We show that the recombination of Cooper pairs in semiconductors can be used as a natural source of polarization-entangled photons, making use of the inherent angular momentum entanglement in the superconducting state. Our proposal is not based on opposite spin population of discrete energy levels and thus does not require isolated emitters such as single atoms or quantum dots. We observe that in bulk materials, the photon entanglement would be degraded due to the variety of decay channels available in the presence of light-hole (LH)–heavy-hole (HH) degeneracy. However, we show that the lifting of this degeneracy by use of a semiconductor quantum well should lead to faithful conversion of the Cooper-pair entanglement into photon entanglement. The second-order decay of two-electron states in Cooper-pair luminescence leaves no which-path information, resulting in perfect coherence between two pathways and hence, in principle, perfect entanglement. We calculate the purity of the entangled-photon state and find that it increases for larger LH–HH energy splitting and for lower temperatures. Moreover, the superconducting macroscopic coherence offers an enhancement to the emission rate, making this a promising scheme for efficient generation of entangled photons in simple electrically driven structures.

DOI: 10.1103/PhysRevB.89.094508 PACS number(s): 74.25.Gz, 42.50.Dv, 03.67.Bg

I. INTRODUCTION

Entanglement is among the most intriguing aspects of quantum mechanics, contradicting the local realism of classical physics via the violation of Bell inequalities [1,2]. Moreover, various applications in the growing field of quantum information science, such as quantum cryptography [3], computing [4], and metrology [5], require efficient sources of entangled photon pairs. The most widely used current technique of generating photon pairs—parametric downconversion [2,6]—is limited by the weakness of the nonresonant $\chi^{(2)}$ nonlinearity [7] and requires phase matching and optical excitation, which prevent its integration into compact photonic circuits. A recently observed process of semiconductor two-photon emission [8,9] enables compact electrically pumped photon-pair sources with nanophotonic enhancement [10]; however, the efficiency of such sources is relatively low due to the nonresonant second-order transition. Cascaded emission from biexcitons in semiconductor quantum dots (QD) allows generation of entanglement in miniature devices, where each discrete QD energy level can only be occupied by two fermions with opposite spins [11]. Anisotropic exchange splitting in QDs, however, leaves which-path information and thus significantly complicates entanglement generation [12]. Hybrid devices based on semiconductor-superconductor structures are a rapidly growing field [13–15], including QDs and nanocrystals integrated into Josephson light-emitting diodes [16,17]. These hybrid devices were proposed as enhanced QD entanglement sources [18–20] based on opposite-spin electrons at each discrete energy level. However, these isolated emitters have inherently low emission rates and require sophisticated fabrication methods, carrier injection, and light extraction techniques. More importantly, superconductivity is not required for the generation of entanglement in isolated emitters such as QDs, where discrete levels allow entanglement generation without superconductivity [11,12].

Two-dimensional and bulk semiconductor structures, at the core of the existing semiconductor optoelectronic infrastructure, are significantly simpler and more efficient, and they have been shown lately to result in enhanced electrically driven light emission when combined with superconductors [21–23]. In contrast to QD-based sources, however, the continuum of states in these structures allows population of infinitesimally close states by electrons with the same spin—preventing any polarization correlation between the emitted photons without superconductivity.

Here we show that Cooper-pair electron-spin entanglement provides a unique source of entangled photon pairs in hybrid superconductor-semiconductor quantum well (QW) structures, which cannot be realized without superconductivity. We show that Cooper-pair angular momentum entanglement can be translated into photon polarization entanglement by radiative recombination in a semiconductor structure. Our analysis shows that a bulk semiconductor-based emitter with spin-orbit coupled angular momentum states results in a mixed photon state (not a pure state and thus not maximally entangled) due to the contribution of both light-hole (LH) and heavy-hole (HH) bands. In a two-dimensional QW, on the other hand, pure entangled states are produced due to the lifting of LH-HH degeneracy and angular momentum selection rules. The recombination of a Cooper pair is a second-order transition [23] that leaves no which-path information in the final state, in contrast to a pair of single-particle first-order transitions. We explicitly calculate the density matrices of the emitted photon-pair states. Small LH-HH splitting and high temperatures can

introduce some mixing into the emitted states; nevertheless, for temperatures sufficiently low to maintain superconductivity and for typical QW dimensions, our calculations predict essentially pure entangled photon states. Furthermore, this approach takes advantage of the macroscopic coherence of the superconducting state for enhanced entanglement generation rates in a relatively simple electrically pumped structure.

II. GENERATION OF PHOTON ENTANGLEMENT BASED ON SUPERCONDUCTIVITY

In the presence of the proximity effect, whereby a superconducting state is induced in a semiconductor, the conduction electrons are not independent but rather form a many-body Bardeen-Cooper-Schrieffer (BCS) [24] state yielding macroscopic coherence and enhanced emission [21]. Furthermore, the second-order emission in a BCS state is a two-electron transition resulting in photon-pair emission, in contrast to the single-electron transitions in usual nonlinear optics [2,6–10]. This two-electron second-order process in a coherent BCS state is what enables both pure entangled state generation and high emission rates in the hybrid semiconductor-superconductor QW structure.

We consider a superconducting proximity region induced in a direct band gap semiconductor [21,25], where the superconducting gap 2Δ is in the semiconductor conduction band (CB) with electrons in a BCS state, while the valence band is in the normal state of holes [Fig. 1(a)]. Near the Brillouin zone center, the CB electrons [26] have total spin-orbit coupled angular momentum $J_z = \pm 1/2$. Electrons in Cooper pairs in an s-wave superconductor are in an angular momentum singlet state [24],

$$|\Psi\rangle = \frac{1}{\sqrt{2}}(|\uparrow\rangle_1|\downarrow\rangle_2 - |\downarrow\rangle_1|\uparrow\rangle_2), \tag{1}$$

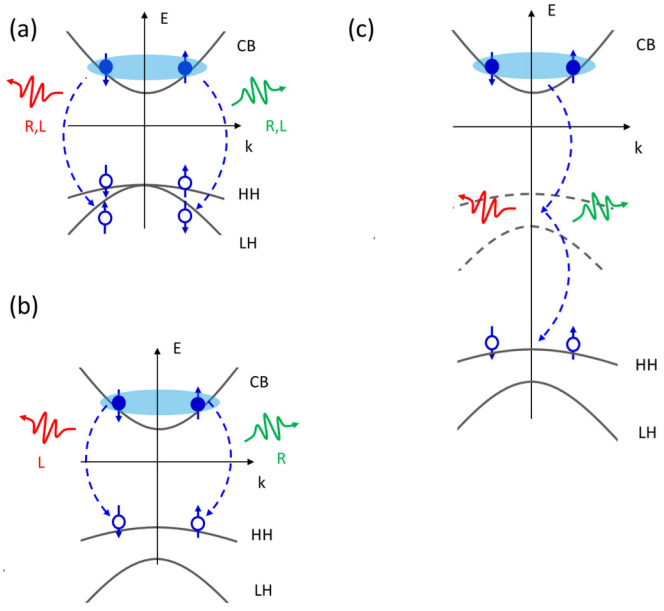

FIG. 1. (Color online) Energy level diagram of Cooper-pair luminescence in a direct band gap semiconductor in the (incorrect) one-particle picture: (a) bulk, (b) QW. (c) Energy-level diagram of Cooper-pair luminescence in a QW in the correct two-particle picture.

where the $|\uparrow\rangle$ and $|\downarrow\rangle$ denote electron states with $J_z = 1/2$ and $J_z = -1/2$, respectively. Recombination of such singlet states in a semiconductor with normal holes, however, does not necessarily result in the emission of entangled photon pairs. The two valence bands with significant populations of holes in typical direct band gap semiconductors—the LH band with $J_z = \pm 1/2$ and the HH band with $J_z = \pm 3/2$—are degenerate at zero crystal momentum. The selection rules for recombination of a HH and a CB electron allow transitions only with an angular momentum change of $\Delta J_z = \pm 1$ [26]. For a singlet CB electron Cooper-pair state, such transitions should result in polarization-correlated photon pairs. However, the presence of the second energy-degenerate LH band with additional allowed transitions degrades polarization correlations [Fig. 1(a)].

In our proposed scheme, the superconducting state is induced in a semiconductor QW, where the LH-HH degeneracy is lifted [Fig. 1(b)]. The two-dimensional QW structures enable injection of a very large number of Cooper pairs, resulting in carrier densities comparable to bulk materials—in contrast to the isolated zero-dimensional QDs. The macroscopic coherence of the BCS state can enhance the emission rate even further [21]. The CB-HH recombination emission results in polarization-correlated photons; however, for polarization *entanglement* to result, there must also be no which-path information in the final state. In a naïve single-particle description of Cooper-pair recombination, the final state might appear to maintain information on the recombination paths of each electron-hole pair, where the angular momentum of each electron-hole pair appears to be translated to a well-defined photon polarization [Fig. 1(b)]. This picture, however, which describes Cooper-pair recombination as two separate first-order transitions, is incorrect because no single-electron states exist inside the superconducting gap at the Fermi level. An electron Cooper pair, therefore, must recombine with a pair of holes in one second-order transition via a virtual state [Fig. 1(c)]. We show that this second-order transition preserves only the total angular momentum, whereas the polarization of each individual photon is not defined. Thus polarization-correlated photons with undefined individual polarization can be entangled. The photons in the pair are tagged by their colors, $\omega^{ph}_{\mathbf{q}_\mu}$ and $\omega^{ph}_{\mathbf{q}_\nu}$, selected by spectral filtering, and are emitted in the direction of growth of the QW.

In addition to the entangled-photon pair emission, one-photon emission will also occur in the proposed device at an energy given by the band gap $E_{\mathrm{BG}} = (E_{\mathrm{CB}} - E_{\mathrm{HH}})$. The one-photon emission will not result in entangled-photon pairs; however, it can be easily separated from the entangled-photon pair emission using spectral filtering of $\omega^{ph}_{\mathbf{q}_\mu}$ and $\omega^{ph}_{\mathbf{q}_\nu}$. The entangled-photon emission in Cooper-pair recombination is a second-order process occurring via a virtual state [Fig. 1(c)] and not a cascade of one-photon emission events [Fig. 1(b)]. Therefore, only the sum of the energies in the photon pair is fixed by the band gap $\omega^{ph}_{\mathbf{q}_\mu} + \omega^{ph}_{\mathbf{q}_\nu} = 2E_{\mathrm{BG}}$, but this does not determine the energy of each individual photon to be E_{BG}. In a second-order process, the two emitted photons can be at energies very different from that of the one-photon emission $\omega^{ph}_{\mathbf{q}_\mu} = E_{\mathrm{BG}} + \delta E$ and $\omega^{ph}_{\mathbf{q}_\nu} = E_{\mathrm{BG}} - \delta E$ as long as the total energy is conserved $\omega^{ph}_{\mathbf{q}_\mu} + \omega^{ph}_{\mathbf{q}_\nu} = 2E_{\mathrm{BG}}$ [2,6–10]. Therefore, for photons selected at energies $\omega^{ph}_{\mathbf{q}_\mu} = E_{\mathrm{BG}} + \delta E$ and

$\omega^{ph}_{\mathbf{q}_\nu} = E_{\mathrm{BG}} - \delta E$, different from E_{BG} by more than the thermal width kT, there is no corresponding one-photon emission, and thus the entangled photon state will not be affected. We calculate the emitted state explicitly for sufficiently large HH-LH splitting, yielding a pure polarization-entangled state.

III. THEORETICAL MODEL AND RESULTS

In contrast to previous calculations [23], our model includes the entire spin-orbit coupled angular momentum J in the interaction and the polarization σ of the photons. Therefore, the light-matter coupling Hamiltonian in the interaction picture with $\hbar = c = 1$ is

$$H_I = \sum_{\mathbf{k},\mathbf{q},\sigma,J} \left(B_{\mathbf{k},\mathbf{q}} b_{-(\mathbf{k}-\mathbf{q}),-J} c_{\mathbf{k},J+\sigma} a^\dagger_{\mathbf{q},\sigma} + B^*_{\mathbf{k},\mathbf{q}} b^\dagger_{-(\mathbf{k}-\mathbf{q}),-J} c^\dagger_{\mathbf{k},J+\sigma} a_{\mathbf{q},\sigma}\right), \quad (2)$$

where $B_{\mathbf{k},\mathbf{q}}$ is the coupling energy, $b^\dagger_{\mathbf{k},J}$ and $c^\dagger_{\mathbf{k},J}$ are hole and electron creation operators with crystal momentum $\mathbf{k}$ and angular momentum J, and $a^\dagger_{\mathbf{q},\sigma}$ is the photon creation operator with linear momentum $\mathbf{q}$ and polarization σ. The initial state is given by $|\chi_0\rangle = |0\rangle|FS\rangle|\mathrm{BCS}\rangle$, where $|0\rangle$ represents the vacuum of the photon field, $|FS\rangle$ denotes the Fermi sea of holes, and $|\mathrm{BCS}\rangle$ is the electron superconducting BCS state. The hole thermal distribution is accounted for by integration over the Fermi-Dirac distribution. The second-order contribution to the final state is given by $|\chi_t\rangle = \int_{-\infty}^{t} dt_1 \int_{-\infty}^{t_1} dt_2 H_I(t_1) H_I(t_2) |\chi_0\rangle$, where $H_I(t) = e^{iH_0 t} H_I e^{-iH_0 t}$ and $H_0 = \sum_{\mathbf{q},\sigma} \omega^{ph}_q a^\dagger_{\mathbf{q},\sigma} a_{\mathbf{q},\sigma} + \sum_{\mathbf{k},J} \omega_k c^\dagger_{\mathbf{k},J} c_{\mathbf{k},J} + \sum_{\mathbf{k}',J'} \omega'_{k'} b^\dagger_{\mathbf{k}',J'} b_{\mathbf{k}',J'}$. This interaction can be described by two-vertex Feynman diagrams [Fig. 2(a)]. The double-arrowed electron propagators describe the Green functions resulting from nonvanishing $\langle \mathrm{BCS}| c^\dagger_{\mathbf{k}_1,J_1} c^\dagger_{\mathbf{k}_2,J_2} |\mathrm{BCS}\rangle$ terms in the superconducting state [27]. This Green function

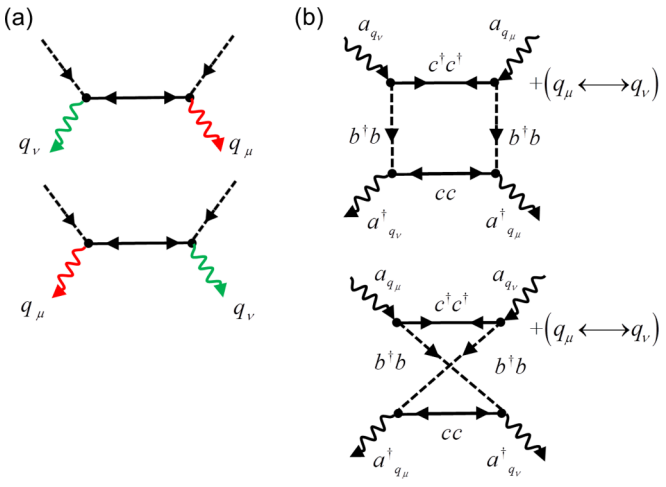

FIG. 2. (Color online) (a) Feynman diagrams of the emission process. The wavy lines indicate photons, dashed lines indicate holes, and the solid lines indicate electrons. The double-arrowed electron propagators describe the Green functions resulting from nonvanishing $\langle \mathrm{BCS}| c^\dagger_{\mathbf{k}_1,J_1} c^\dagger_{\mathbf{k}_2,J_2} |\mathrm{BCS}\rangle$ terms. (b) Feynman diagrams of the density matrix calculations.

permits pair emission through a single connected second-order Feynman diagram, in contrast to the disconnected pair of first-order single-electron transitions. It is important to note that the initial electron state is not a single Cooper pair in a singlet state but rather a many-body BCS state. Therefore, the entangled photon state emitted from the second-order transition does not have to be in a singlet state. The color-specific two-photon polarization state is fully described by the density matrix $\rho(q_\mu, q_\nu)$, whose elements are given by the following expectation value in the final state [12]:

$$\begin{aligned}\rho(q_\mu,q_\nu)_{\sigma_\alpha,\sigma_\beta,\sigma_\gamma,\sigma_\delta} &= \langle\chi_t| a^\dagger_{\mathbf{q}_\mu,\sigma_\alpha} a^\dagger_{\mathbf{q}_\nu,\sigma_\beta} a_{\mathbf{q}_\mu,\sigma_\gamma} a_{\mathbf{q}_\nu,\sigma_\delta} |\chi_t\rangle \\ &= \int_{-\infty}^{t} dt_1 \int_{-\infty}^{t_1} dt_2 \int_{-\infty}^{t} dt_3 \int_{-\infty}^{t_3} dt_4 \langle\chi_0| H_I(t_1) H_I(t_2) \\ &\quad \times a^\dagger_{\mathbf{q}_\mu,\sigma_\alpha} a^\dagger_{\mathbf{q}_\nu,\sigma_\beta} a_{\mathbf{q}_\mu,\sigma_\gamma} a_{\mathbf{q}_\nu,\sigma_\delta} H_I(t_3) H_I(t_4) |\chi_0\rangle . \end{aligned} \quad (3)$$

This calculation can be described by two kinds of Feynman diagrams [Fig. 2(b)], which can be used to obtain the qualitative structure of the density matrix conveniently; however, straight-forward integration enables the quantitative calculation of the amplitudes. The integrand in Eq. (3) can be split into the photon (I_{ph}), electron (I_e), and hole (I_h) terms:

$$\begin{aligned}&\langle\chi_0| H_I(t_1) H_I(t_2) a^\dagger_{\mathbf{q}_\mu,\sigma_\alpha} a^\dagger_{\mathbf{q}_\nu,\sigma_\beta} a_{\mathbf{q}_\mu,\sigma_\gamma} a_{\mathbf{q}_\nu,\sigma_\delta} H_I(t_3) H_I(t_4) |\chi_0\rangle \\ &= \sum_{\mathbf{k}_1..\mathbf{k}_4,\mathbf{q}_1..\mathbf{q}_4,\sigma_1..\sigma_4,J_1..J_4} B^*_{\mathbf{k}_1,\mathbf{q}_1} B^*_{\mathbf{k}_2,\mathbf{q}_2} B_{\mathbf{k}_3,\mathbf{q}_3} B_{\mathbf{k}_4,\mathbf{q}_4} I_{ph} I_h I_e \\ &\quad \times e^{-i(\omega^{ph}_{\mathbf{q}_1} - \omega_{\mathbf{k}_1-\mathbf{q}_1})t_1} e^{-i(\omega^{ph}_{\mathbf{q}_2} - \omega_{\mathbf{k}_2-\mathbf{q}_2})t_2} \\ &\quad \times e^{i(\omega^{ph}_{\mathbf{q}_3} - \omega_{\mathbf{k}_3-\mathbf{q}_3})t_3} e^{i(\omega^{ph}_{\mathbf{q}_4} - \omega_{\mathbf{k}_4-\mathbf{q}_4})t_4}. \end{aligned} \quad (4)$$

The photon term is calculated to be

$$\begin{aligned} I_{ph} = \big(&\delta_{\sigma_1,\sigma_\beta}\delta_{\sigma_2,\sigma_\alpha}\delta_{\sigma_3,\sigma_\delta}\delta_{\sigma_4,\sigma_\gamma}\delta_{\mathbf{q}_1,\mathbf{q}_\nu}\delta_{\mathbf{q}_2,\mathbf{q}_\mu}\delta_{\mathbf{q}_3,\mathbf{q}_\nu}\delta_{\mathbf{q}_4,\mathbf{q}_\mu} \\ &+ \delta_{\sigma_1,\sigma_\alpha}\delta_{\sigma_2,\sigma_\beta}\delta_{\sigma_3,\sigma_\delta}\delta_{\sigma_4,\sigma_\gamma}\delta_{\mathbf{q}_1,\mathbf{q}_\mu}\delta_{\mathbf{q}_2,\mathbf{q}_\nu}\delta_{\mathbf{q}_3,\mathbf{q}_\nu}\delta_{\mathbf{q}_4,\mathbf{q}_\mu} \\ &+ \delta_{\sigma_1,\sigma_\beta}\delta_{\sigma_2,\sigma_\alpha}\delta_{\sigma_3,\sigma_\gamma}\delta_{\sigma_4,\sigma_\delta}\delta_{\mathbf{q}_1,\mathbf{q}_\nu}\delta_{\mathbf{q}_2,\mathbf{q}_\mu}\delta_{\mathbf{q}_3,\mathbf{q}_\mu}\delta_{\mathbf{q}_4,\mathbf{q}_\nu} \\ &+ \delta_{\sigma_1,\sigma_\alpha}\delta_{\sigma_2,\sigma_\beta}\delta_{\sigma_3,\sigma_\gamma}\delta_{\sigma_4,\sigma_\delta}\delta_{\mathbf{q}_1,\mathbf{q}_\mu}\delta_{\mathbf{q}_2,\mathbf{q}_\nu}\delta_{\mathbf{q}_3,\mathbf{q}_\mu}\delta_{\mathbf{q}_4,\mathbf{q}_\nu}\big), \end{aligned} \quad (5)$$

and the hole term is

$$\begin{aligned} I_h = f^p_{\mathbf{k}_i} f^p_{\mathbf{k}_j} \big(&\delta_{\mathbf{k}_1-\mathbf{q}_1,\mathbf{k}_3-\mathbf{q}_3}\delta_{J_1,J_3}\delta_{\mathbf{k}_2-\mathbf{q}_2,\mathbf{k}_4-\mathbf{q}_4}\delta_{J_2,J_4} \\ &- \delta_{\mathbf{k}_1-\mathbf{q}_1,\mathbf{k}_4-\mathbf{q}_4}\delta_{J_1,J_4}\delta_{\mathbf{k}_2-\mathbf{q}_2,\mathbf{k}_3-\mathbf{q}_3}\delta_{J_2,J_3}\big), \end{aligned} \quad (6)$$

where $f^p_{\mathbf{k}_i}$ and $f^p_{\mathbf{k}_j}$ are Fermi-Dirac population distributions for holes with momenta $\mathbf{k}_i$ and $\mathbf{k}_j$, respectively. The Cooper-pair electron term is calculated in a BCS state $I_e = \langle \mathrm{BCS}| c^\dagger_{\mathbf{k}_1,J_1+\sigma_1}(t_1) c^\dagger_{\mathbf{k}_2,J_2+\sigma_2}(t_2) c_{\mathbf{k}_3,J_3+\sigma_3}(t_3) c_{\mathbf{k}_4,J_4+\sigma_4}(t_4)|\mathrm{BCS}\rangle$ using the Bogoliubov transformation

$$c^\dagger_{\mathbf{k},J}(t) = e^{i\tilde{\mu}_n t}(u_{\mathbf{k}} e^{iE_{\mathbf{k}}t} \gamma^\dagger_{\mathbf{k},J} - s_J v_{\mathbf{k}} e^{-iE_{\mathbf{k}}t} \gamma_{-\mathbf{k},-J}), \quad (7)$$

where $\gamma^\dagger_{\mathbf{k},J}$ is a Bogoliubov quasiparticle creation operator with crystal momentum $\mathbf{k}$ and angular momentum J, the electron energy above the quasi Fermi level, E_{Fn}, is $\xi_n(\mathbf{k}) = \mathbf{k}^2/2m_n - E_{Fn}$, and quasiparticle energy is $E_{\mathbf{k}} = \sqrt{\xi^2_n(\mathbf{k}) + \Delta^2}$, $\tilde{\mu}_n = E_{\mathrm{CB}} + E_{Fn}$, $s_J = 1(-1)$ for $J = \uparrow(\downarrow)$, and $u_{\mathbf{k}} = \sqrt{1/2\,[1 + \xi_n(\mathbf{k})/E_{\mathbf{k}}]}$ and $v_{\mathbf{k}} = \sqrt{1/2[1 - \xi_n(\mathbf{k})/E_{\mathbf{k}}]}$. The Cooper-pair electron term

is then

$$I_e = u_{\mathbf{k}_1} v_{\mathbf{k}_1} u^*_{\mathbf{k}_3} v^*_{\mathbf{k}_3} \delta_{\mathbf{k}_1, J_1+\sigma_1, -\mathbf{k}_2, -(J_2+\sigma_2)} \delta_{-\mathbf{k}_3, -(J_3+\sigma_3), \mathbf{k}_4, J_4+\sigma_4} s_{J_1+\sigma_1} s_{J_3+\sigma_3} e^{i\tilde{\mu}_n t_1} e^{i\tilde{\mu}_n t_2} e^{-i\tilde{\mu}_n t_3} e^{-i\tilde{\mu}_n t_4} \left(e^{iE_{\mathbf{k}_1}(t_1-t_2)} e^{-iE_{\mathbf{k}_3}(t_3-t_4)} f^n_{\mathbf{k}_1} \left(1 - f^n_{\mathbf{k}_3}\right) \right.$$
$$\left. + e^{-iE_{\mathbf{k}_1}(t_1-t_2)} e^{iE_{\mathbf{k}_3}(t_3-t_4)} f^n_{\mathbf{k}_3} \left(1 - f^n_{\mathbf{k}_1}\right) - e^{-iE_{\mathbf{k}_1}(t_1-t_2)} e^{-iE_{\mathbf{k}_3}(t_3-t_4)} \left(1 - f^n_{\mathbf{k}_1}\right)\left(1 - f^n_{\mathbf{k}_3}\right) - e^{iE_{\mathbf{k}_1}(t_1-t_2)} e^{iE_{\mathbf{k}_3}(t_3-t_4)} f^n_{\mathbf{k}_1} f^n_{\mathbf{k}_3} \right), \quad (8)$$

where $f^n_{\mathbf{k}}$ is the Fermi-Dirac population distribution. For the HH band only, and assuming that $f^n_{\mathbf{k}}$ and $u_{\mathbf{k}}$ are slowly varying on the scale of $\mathbf{q}$, the density matrix is

$$\rho(q_\mu, q_\nu)^{\mathrm{HH}}$$
$$= \sum_{\mathbf{k}} \pi \left|B_{\mathbf{k},\mathbf{q}_\mu}\right|^2 \left|B_{\mathbf{k},\mathbf{q}_\nu}\right|^2 |\Delta_{\mathbf{k}}/E_{\mathbf{k}}|^2 \left(f^p_{\mathbf{k}}\right)^2 \delta\left(\omega^{ph}_{\mathbf{q}_\nu} + \omega^{ph}_{\mathbf{q}_\mu} - 2\omega_{\mathbf{k}} - 2\tilde{\mu}_n\right) \begin{pmatrix} 0 & 0 & 0 & 0 \\ 0 & 1 & 1 & 0 \\ 0 & 1 & 1 & 0 \\ 0 & 0 & 0 & 0 \end{pmatrix} \left(\frac{f^n_{\mathbf{k}}\left(1 - f^n_{\mathbf{k}}\right)}{\left(E_{\mathbf{q}_\mu,\mathbf{k}} + E_{\mathbf{k}}\right)^2} + \frac{f^n_{\mathbf{k}}\left(1 - f^n_{\mathbf{k}}\right)}{\left(E_{\mathbf{q}_\mu,\mathbf{k}} - E_{\mathbf{k}}\right)^2} \right.$$
$$- \frac{\left(1 - f^n_{\mathbf{k}}\right)\left(1 - f^n_{\mathbf{k}}\right)}{\left(E_{\mathbf{q}_\mu,\mathbf{k}} - E_{\mathbf{k}}\right)\left(E_{\mathbf{q}_\mu,\mathbf{k}} + E_{\mathbf{k}}\right)} - \frac{f^n_{\mathbf{k}} f^n_{\mathbf{k}}}{\left(E_{\mathbf{q}_\mu,\mathbf{k}} + E_{\mathbf{k}}\right)\left(E_{\mathbf{q}_\mu,\mathbf{k}} - E_{\mathbf{k}}\right)} + \frac{f^n_{\mathbf{k}}\left(1 - f^n_{\mathbf{k}}\right)}{\left(E_{\mathbf{q}_\nu,\mathbf{k}} + E_{\mathbf{k}}\right)\left(E_{\mathbf{q}_\mu,\mathbf{k}} + E_{\mathbf{k}}\right)}$$
$$\left. + \frac{f^n_{\mathbf{k}}\left(1 - f^n_{\mathbf{k}}\right)}{\left(E_{\mathbf{q}_\nu,\mathbf{k}} - E_{\mathbf{k}}\right)\left(E_{\mathbf{q}_\mu,\mathbf{k}} - E_{\mathbf{k}}\right)} - \frac{\left(1 - f^n_{\mathbf{k}}\right)\left(1 - f^n_{\mathbf{k}}\right)}{\left(E_{\mathbf{q}_\nu,\mathbf{k}} - E_{\mathbf{k}}\right)\left(E_{\mathbf{q}_\mu,\mathbf{k}} + E_{\mathbf{k}}\right)} - \frac{f^n_{\mathbf{k}} f^n_{\mathbf{k}}}{\left(E_{\mathbf{q}_\nu,\mathbf{k}} + E_{\mathbf{k}}\right)\left(E_{\mathbf{q}_\mu,\mathbf{k}} - E_{\mathbf{k}}\right)} + (\mathbf{q}_\mu \leftrightarrow \mathbf{q}_\nu) \right), \quad (9)$$

where $E_{\mathbf{q}_\mu,\mathbf{k}} = \omega^{ph}_{\mathbf{q}_\mu} - \omega_{\mathbf{k}} - \tilde{\mu}_n$, $E_{\mathbf{q}_\nu,\mathbf{k}} = \omega^{ph}_{\mathbf{q}_\nu} - \omega_{\mathbf{k}} - \tilde{\mu}_n$, and $(\mathbf{q}_\mu \leftrightarrow \mathbf{q}_\nu)$ indicates another eight terms similar to the first eight but with exchanged q_μ and q_ν. The basis for the two-photon density matrix is circular right- or left-handed polarization $|R_{\mathbf{q}_\mu} R_{\mathbf{q}_\nu}\rangle, |R_{\mathbf{q}_\mu} L_{\mathbf{q}_\nu}\rangle, |L_{\mathbf{q}_\mu} R_{\mathbf{q}_\nu}\rangle, |L_{\mathbf{q}_\mu} L_{\mathbf{q}_\nu}\rangle$. The two-photon state is not only polarization correlated but is in fact a pure entangled state:

$$|\Psi_{ph}\rangle = \frac{1}{\sqrt{2}}\left(\left|R_{\mathbf{q}_\mu} L_{\mathbf{q}_\nu}\right\rangle + \left|L_{\mathbf{q}_\mu} R_{\mathbf{q}_\nu}\right\rangle\right). \quad (10)$$

This entangled state is a result of the correlated photon polarization with no which-path information; however, the plus sign in Eq. (10) is different from the minus sign in the singlet state in Eq. (1). The reason for this difference is the effect of the many-body antisymmetrization in the BCS state. This calculation result is also validated by the Feynman diagram approach. Each diagram in Fig. 2(b) corresponds to one of the terms in the expression for the hole part of the calculation, I_h [Eq. (6)], and the negative sign between the first and second terms results from the fermionic exchange of holes [Fig. 2(b), dashed lines]. In the density matrix [Eq. (9)], the nonvanishing diagonal elements are described by the first diagram in Fig. 2(b) and the off-diagonal elements by the second diagram. However, the sign of the off-diagonal elements in Eq. (9) is changed due to the minus sign in the Bogoliubov transformation [Eq. (7)] so that all four elements are positive. Conservation of angular momentum at each vertex of the diagrams then allows the determination of the photon polarization similar to the nonvanishing elements of the calculated density matrix [Eq. (9)].

In a bulk semiconductor, the LH band adds other nonvanishing elements to the density matrix thus resulting in a mixed state [Fig. 3(a)],

$$\rho(q_\mu, q_\nu) = \alpha\rho(q_\mu, q_\nu)^{\mathrm{HH}} + \beta\rho(q_\mu, q_\nu)^{\mathrm{LH}}, \quad (11)$$

where $\rho(q_\mu, q_\nu)^{\mathrm{LH}}$ is the contribution of the LH-CB transitions with nonvanishing elements corresponding to photons with identical circular polarization, and the coefficients α and β depend on the population of the bands according to Eq. (9). The dipole moments of CB-LH transitions in direct band gap (e.g., Zincblende) materials are different from those of CB-HH [26]; therefore, even for a bulk semiconductor with LH-HH degeneracy, the emitted two-photon state is not completely mixed. However, in a QW with a much smaller population of the LH band the purity of the state [Eq. (11)] is enhanced [Fig. 3(b)].

IV. DISCUSSION

The purity of the generated entangled states, therefore, relies on the interplay between energy scales of the LH-HH splitting due to spin-orbit interaction (SOI), semiconductor band gap, injected carrier density, and the temperature. The largest energy scale in this scheme is the band gap between the conduction E_{CB} and the valence $E_{\mathrm{HH\text{-}LH}}$ bands, which determines the energy of the emitted photons. In typical AlGaAs structures, the band gap is larger than 1500 meV [28] and is therefore much larger than all other energy scales in the system. The SOI in GaAs-based materials is significant but much smaller than the band gap. In bulk GaAs, the split-off band is 340 meV below the top valence band [29]. The SOI energy ΔE_{SOI} is thus smaller than the band gap but larger than other energies in our system. The superconducting gap, Δ, induced in semiconductors by typical low T_c superconductors such as Nb is on the meV scale [30] so that $E_{\mathrm{CB}} - E_{\mathrm{HH\text{-}LH}} \gg \Delta E_{\mathrm{SOI}} \gg E_{\mathrm{HH}} - E_{\mathrm{LH}}, E_{Fp} - E_{\mathrm{LH}}, E_{Fn} - E_{\mathrm{CB}} \gg \Delta$. The injected electron and hole densities determine the locations of the conduction and the valence band quasi Fermi levels relative to the band edges: $E_{Fn} - E_{\mathrm{CB}}$, $E_{Fp} - E_{\mathrm{HH}}$, and $E_{Fp} - E_{\mathrm{LH}}$. At practical injection levels in typical optoelectronic materials such as AlGaAs, this energy scale is around 10 meV and can be calculated with analytical approximations [31]. The populations of the LH and the HH bands depend on the $\Delta E_H = E_{\mathrm{HH}} - E_{\mathrm{LH}}$ energy splitting determined by the thickness of the QW reaching values of tens of meV [29]. For a fixed

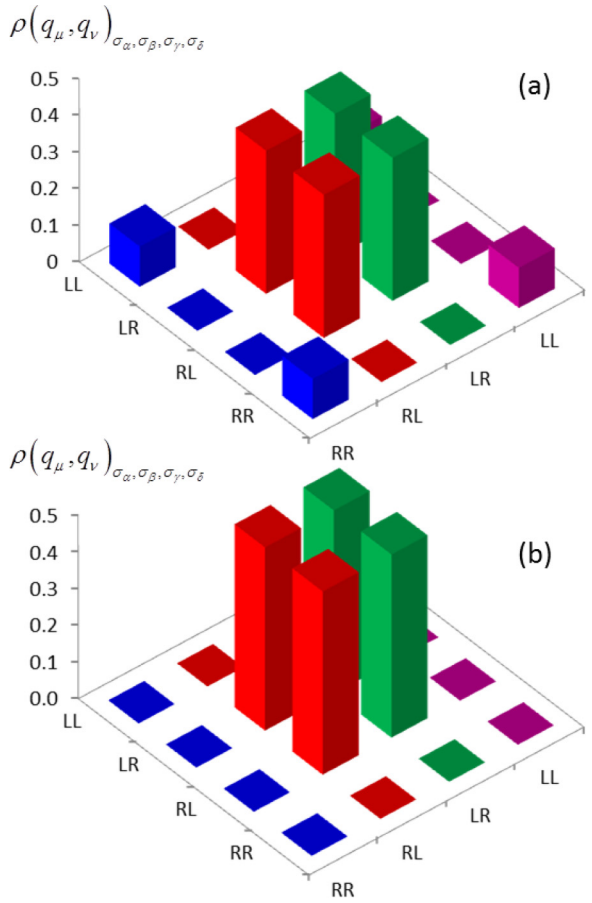

FIG. 3. (Color online) Calculated density matrix of the two-photon polarization state for Cooper-pair luminescence in (a) a bulk direct band gap semiconductor and (b) a QW with large LH-HH splitting.

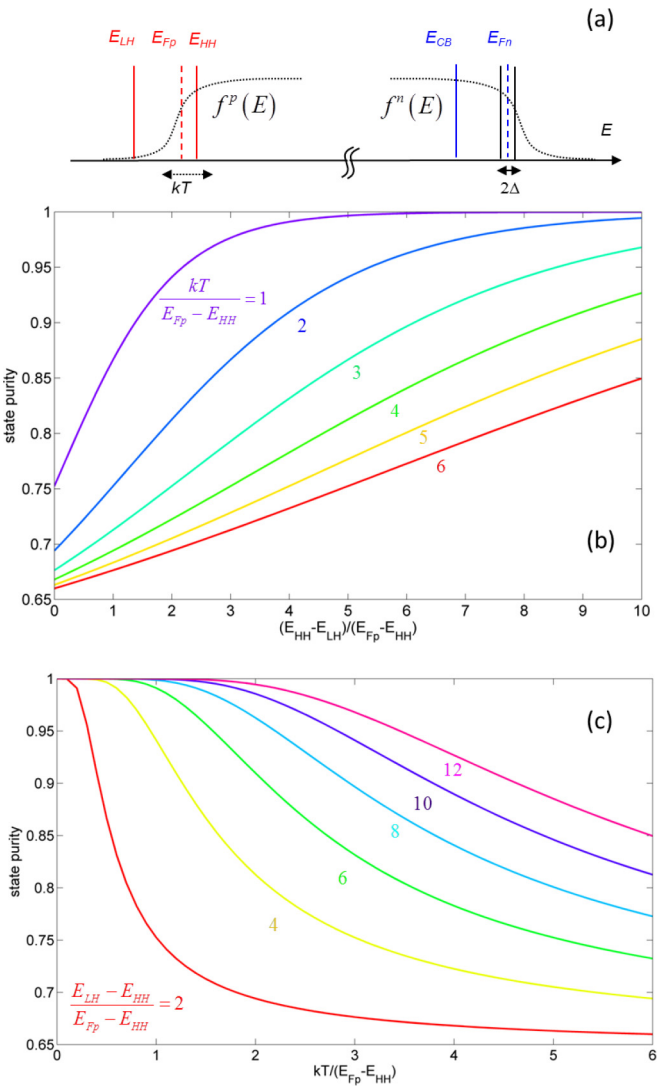

FIG. 4. (Color online) (a) A schematic diagram of the energy scales. The solid lines indicate band edge energies, the dashed lines indicate quasi Fermi levels, and the dotted curves indicate the Fermi-Dirac population distributions. (b), (c) Calculated purity of the photon polarization-entangled state (b) vs LH-HH energy splitting for different temperatures (c) vs temperature for different LH-HH energy splitting, where $E_{\rm LH}$ and $E_{\rm HH}$ are LH and HH band edge energies respectively, E_{Fp} is the valence band quasi Fermi level, and T is the temperature.

carrier injection level and a given LH-HH splitting, the hole populations of the HH and the LH bands depend on temperature according to the Fermi-Dirac distribution $f^p(E)$ [Fig. 4(a)]. High purity of the emitted entangled photons is obtained by reducing the LH contribution $\rho(q_\mu,q_\nu)^{\rm LH}$ in Eq. (11), which can be obtained by lowering the temperature or by increasing the LH-HH splitting.

Typical LH-HH splitting in a QW can result in an entangled state with very high purity, whereas at smaller LH-HH splitting, ΔE_H, the holes partially populate both HH and LH bands. For lower temperature, T, the population of the LH band is smaller, and the CB-LH transition degrades the entangled state purity, given by $Tr[\rho(q_\mu,q_\nu)^2]$, less severely than at higher temperatures [Fig. 4(c)]. Nevertheless, even at higher temperatures, high purity of entanglement can be obtained by increasing the LH-HH separation [Fig. 4(b)]. In typical semiconductor QWs used in optoelectronics, the LH-HH separation of several tens of meV can be obtained for QW thickness smaller than 10 nm [29]. Therefore, mixing of the entangled states will be significant only close to room temperature. At temperatures below the superconducting transition of typical s-wave low-T_c materials such as Nb [30], the emitted photons thus should be in an essentially pure entangled state. The superconducting proximity effect has been demonstrated recently with high-T_c materials [32], enabling potential applications of this scheme at much higher temperatures in hybrid semiconductor high-T_c devices as well [33].

Another effect that could hinder the proper operation of the proposed device is strong disorder. Disorder-induced levels can lead to one-photon emission with energies above the band gap $E_{\rm BG}$ by normal electron-hole recombination. They can also lead to one-photon emission with energies below $E_{\rm BG}$ by recombination of a Cooper pair with a single hole, which results in a photon and an electron at a higher energy level. If the two-photon emission is selected at energies similar to those of the disorder-induced one-photon emission, the quality of the entanglement source can be affected. As the overall

second-order Cooper-pair recombination rate has been shown to be comparable to the first-order normal recombination rate [21–23], this effect of the disorder-induced one-photon emission on the source quality is limited.

However, to prevent even the small effect of disorder-induced emission and ensure perfect operation of the device, the energy difference of the photons in the pair must be larger than the energy broadening given by the disorder ΔE_D so that photon-pair emission can be spectrally filtered from disorder-induced one-photon emission. The energy broadening of the one-photon emission is limited by the level of the disorder in the system, whereas the desired energy difference between the photons in the entangled pair is limited by the separation between the LH and HH energies ΔE_H to ensure the generation of pure entangled states. It is important to note that even at energies where two-photon emission intensity is comparable to the disorder-induced one-photon emission intensity, the one-photon emission still does not pose an obstacle to exploiting the entangled photon pairs. Quantum information experiments using entangled photons are based on photon coincidences. The correlated two-photon emission, even at energies where it is comparable in intensity with the background one-photon emission, results in significantly higher photon coincidence rates than the random one-photon emission, making the effect of such background one-photon emission on quantum information experiments negligible.

Nevertheless, in order to demonstrate the spectral filtering of the two-photon emission quantitatively, we have calculated the intensity spectrum of the two-photon emission at zero temperature [Eq. (12)]:

$$I \propto \left|\frac{\Delta}{\Omega}\right|^2 \left(\frac{1}{\left(\omega^{ph}_{\mathbf{q}_\mu} - \omega^{ph}_{\mathbf{q}_\nu}\right)^2 - \Omega^2} + \frac{1}{\left(\omega^{ph}_{\mathbf{q}_\nu} - \omega^{ph}_{\mathbf{q}_\mu} + \Omega\right)\left(\omega^{ph}_{\mathbf{q}_\mu} - \omega^{ph}_{\mathbf{q}_\nu} - \Omega\right)} \right.$$
$$\left. + \frac{1}{\left(\omega^{ph}_{\mathbf{q}_\nu} - \omega^{ph}_{\mathbf{q}_\mu}\right)^2 - \Omega^2} + \frac{1}{\left(\omega^{ph}_{\mathbf{q}_\mu} - \omega^{ph}_{\mathbf{q}_\nu} + \Omega\right)\left(\omega^{ph}_{\mathbf{q}_\nu} - \omega^{ph}_{\mathbf{q}_\mu} - \Omega\right)} \right), \tag{12}$$

where $\Omega = \sqrt{(\omega^{ph}_{\mathbf{q}_\nu} + \omega^{ph}_{\mathbf{q}_\mu} - 2\tilde{\mu}_n)^2 + 4\Delta^2}$.

The calculated spectrum of the two-photon emission (Fig. 5) exhibits a power-law energy dependence of the intensity at energies above Δ, compared to the significantly steeper drop in the spectrum of the parasitic one-photon emission from the typical Gaussian distribution of disorder-induced energy levels in epitaxial QWs [34]. In modern high quality AlGaAs QWs, the thickness variation can be controlled on a monolayer level, resulting in very narrow line widths of around $\Delta E_D \sim 0.5$ meV, which ensures the desired conditions: $\Delta E_D \ll \Delta E_H$ and $\Delta E_D \ll \Delta$. This narrow line width also enables strongly coupled light-matter interaction in microcavities and was measured both spectrally [35] and with ultrafast pump-probe experiments [36]. For such levels of disorder, it can be seen that for photon energies detuned by more than Δ from the transition energy, the two-photon intensity is higher than the disorder-induced one-photon emission intensity—by many orders of magnitude (Fig. 5). Nonzero temperature adds broadening on the order of kT to the spectra; however, this broadening has little effect on the intensity difference, especially for temperatures sufficiently low to maintain superconductivity $kT \ll \Delta$. Very high levels of disorder can also potentially hinder the induced superconductivity in the semiconductor. However, the typical disorder broadening of line shapes in high quality extended two-dimensional structures such as the QW in our scheme can be smaller than 0.5 meV [35,36], whereas the typical superconducting gaps in low-T_c materials can be an order of magnitude larger than that. And in high-T_c materials, the gap can be several orders of magnitude larger [32]. Therefore, for devices based on typical QWs, disorder-induced one-photon emission does not affect the operation of the proposed device, and for low quality structures, the disorder-induced broadening should be smaller than the superconducting gap for proper operation of the device.

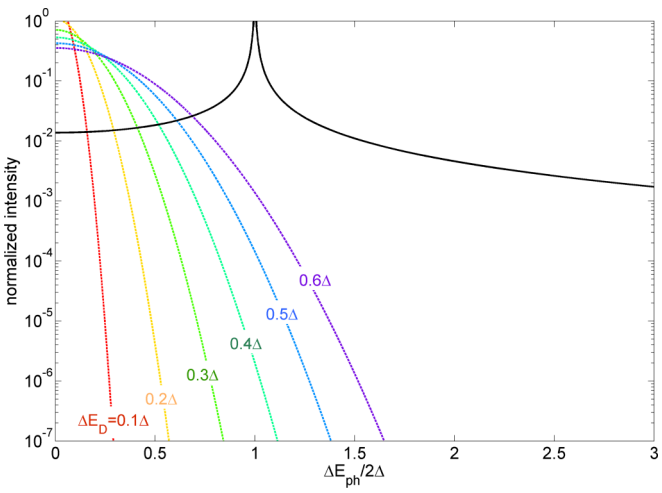

FIG. 5. (Color online) Calculated spectrum of the two-photon emission (solid black line) and the disorder-induced one-photon emission for different values of disorder broadening ΔE_D (dashed lines). $\Delta E_{ph}/2$ is the detuning of the photons from the transition energy.

V. CONCLUSIONS

In conclusion, we have shown that polarization-entangled photons can be generated by Cooper-pair luminescence in semiconductors without isolated emitters. Due to the lack of which-path information in the second-order transition and the lifted degeneracy of the valence bands in QWs, the emission results in pure-state polarization-entangled photons, with generation rates enhanced by the macroscopic coherence

of the superconducting state. The proposed source of entangled photons can provide insights into the physics of superconductivity and light-matter interaction in solids, as well as enable practical applications in quantum technologies.

ACKNOWLEDGMENTS

We appreciate financial support from the Natural Sciences and Engineering Research Council of Canada (NSERC) and from the Canadian Institute for Advanced Research (CIFAR).

[1] G. Weihs, T. Jennewein, C. Simon, H. Weinfurter, and A. Zeilinger, Phys. Rev. Lett. **81**, 5039 (1998).
[2] P. G. Kwiat, K. Mattle, H. Weinfurter, A. Zeilinger, A. V. Sergienko, and Y. Shih, Phys. Rev. Lett. **75**, 4337 (1995).
[3] N. Gisin, G. Ribordy, W. Tittel, and H. Zbinden, Rev. Mod. Phys. **74**, 145 (2002); T. Jennewein, C. Simon, G. Weihs, H. Weinfurter, and A. Zeilinger, Phys. Rev. Lett. **84**, 4729 (2000).
[4] J. L. O'Brien, Science **318**, 1567 (2007); T. D. Ladd, F. Jelezko, R. Laflamme, Y. Nakamura, C. Monroe, and J. L. O'Brien, Nature **464**, 45 (2010).
[5] T. Nagata, R. Okamoto, J. L. O'Brien, K. Sasaki, and S. Takeuchi, Science **316**, 726 (2007); M. W. Mitchell, J. S. Lundeen, and A. M. Steinberg, Nature **429**, 161 (2004).
[6] A. G. White, D. F. V. James, P. H. Eberhard, and P. G. Kwiat, Phys. Rev. Lett. **83**, 3103 (1999).
[7] R. W. Boyd, *Nonlinear Optics*, 3rd ed. (Academic Press, London, U. K., 2008).
[8] A. Hayat, P. Ginzburg, and M. Orenstein, Nature Photon. **2**, 238 (2008); Phys. Rev. Lett. **103**, 023601 (2009).
[9] Y. Ota, S. Iwamoto, N. Kumagai, and Y. Arakawa, Phys. Rev. Lett. **107**, 233602 (2011).
[10] A. N. Poddubny, P. Ginzburg, P. A. Belov, A. V. Zayats, and Y. S. Kivshar, Phys. Rev. A **86**, 033826 (2012); A. Nevet, N. Berkovitch, A. Hayat, P. Ginzburg, S. Ginzach, O. Sorias, and M. Orenstein, Nano Lett. **10**, 1848 (2010).
[11] R. M. Stevenson, R. J. Young, P. Atkinson, K. Cooper, D. A. Ritchie, and A. J. Shields, Nature **439**, 179 (2006); Akopian, N. H. Linder, E. Poem, Y. Berlatzky, J. Avron, D. Gershoni, B. D. Geradot, and P. M. Petroff, Phys. Rev. Lett. **96**, 130501 (2006).
[12] E. A. Meirom, N. H. Lindner, Y. Berlatzky, E. Poem, N. Akopian, J. E. Avron, and D. Gershoni, Phys. Rev. A **77**, 062310 (2008).
[13] S. De Franceschi, L. Kouwenhoven, C. Schönenberger, and W. Wernsdorfer, Nature Nanotech. **5**, 703 (2010).
[14] G. Katsaros, P. Spathis, M. Stoffel, F. Fournel, M. Mongillo, V. Bouchiat, F. Lefloch, A. Rastelli, O. G. Schmidt, and S. De Franceschi, Nature Nanotech. **5**, 458 (2010).
[15] V. Mourik, K. Zuo, S. M. Frolov, S. R. Plissard, E. P. A. M. Bakkers, and L. P. Kouwenhoven, Science, **336**, 1003 (2012).
[16] P. Recher, Y. V. Nazarov, and L. P. Kouwenhoven, Phys. Rev. Lett. **104**, 156802 (2010).
[17] F. Godschalk, F. Hassler, and Y. V. Nazarov, Phys. Rev. Lett. **107**, 073901 (2011).
[18] I. Suemune, T. Akazaki, K. Tanaka, M. Jo, K. Uesugi, M. Endo, H. Kumano, E. Hanamura, H. Takayanagi, M. Yamanishi, and H. Kan, Jpn. J. Appl. Phys. **45**, 9264 (2006).
[19] F. Hassler, Y. V. Nazarov, and L. P. Kouwenhoven, Nanotechnology **21**, 274004 (2010).
[20] M. Khoshnegar and A. H. Majedi, Phys. Rev. B **84**, 104504 (2011).
[21] H. Sasakura, S. Kuramitsu, Y. Hayashi, K. Tanaka, T. Akazaki, E. Hanamura, R. Inoue, H. Takayanagi, Y. Asano, C. Hermannstädter, H. Kumano, and I. Suemune, Phys. Rev. Lett. **107**, 157403 (2011).
[22] I. Suemune, Y. Hayashi, S. Kuramitsu, K. Tanaka, T. Akazaki, H. Sasakura, R. Inoue, H. Takayanagi, Y. Asano, E. Hanamura, S. Odashima, and H. Kumano, Appl. Phys. Express **3**, 054001 (2010).
[23] Y. Asano, I. Suemune, H. Takayanagi, and E. Hanamura, Phys. Rev. Lett. **103**, 187001 (2009).
[24] M. Tinkham, *Introduction to Superconductivity*, 2nd ed. (McGraw-Hill, New York, 1996).
[25] A. Kastalsky, A. W. Kleinsasser, L. H. Greene, R. Bhat, F. P. Milliken, and J. P. Harbison, Phys. Rev. Lett. **67**, 3026 (1991).
[26] C. C. Lee and H. Y. Fan, Phys. Rev. B **9**, 3502 (1974).
[27] A. A. Abrikosov, L. P. Gorkov, and I. E. Dzyaloshinski, *Methods of Quantum Field Theory in Statistical Physics* (Prentice Hall, Englewood Cliffs, NJ, 1963).
[28] A. K. Saxena, J. Phys. C. **13**, 4323 (1980).
[29] G. Bastard, *Wave Mechanics Applied to Semiconductor Heterostructures* (Wiley-Interscience, Paris, 1991).
[30] D. R. Heslinga, S. E. Shafranjuk, H. van Kempen, and T. M. Klapwijk, Phys. Rev. B **49**, 10484 (1994).
[31] W. B. Joyce and R. W. Dixon, Appl. Phys. Lett. **31**, 354 (1977).
[32] P. Zareapour, A. Hayat, S. Y. F. Zhao, M. Kreshchuk, A. Jain, D. C. Kwok, N. Lee, S.-W. Cheong, Z. Xu, A. Yang, G. D. Gu, R. J. Cava, and K. S. Burch, Nature Commun. **3**, 1056 (2012).
[33] A. Hayat, P. Zareapour, S. Y. F. Zhao, A. Jain, I. G. Savelyev, M. Blumin, Z. Xu, A. Yang, G. D. Gu, H. E. Ruda, S. Jia, R. J. Cava, A. M. Steinberg, and K. S. Burch, Phys. Rev. X **2**, 041019 (2012).
[34] M. A. Herman, D. Bimberg, and J. Christen, J. Appl. Phys. **70**, R1 (1991); D. Bimberg, D. Mars, J. N. Miller, R. Bauer, and D. Oertel, J. Vac. Sci. Technol. B **4**, 1014 (1986).
[35] H. M. Gibbs, G. Khitrova, and S. W. Koch, Nature Photon. **5**, 273 (2011).
[36] A. Hayat, C. Lange, L. A. Rozema, A. Darabi, H. M. van Driel, A. M. Steinberg, B. Nelsen, D. W. Snoke, L. N. Pfeiffer, and K. W. West, Phys. Rev. Lett. **109**, 033605 (2012).